Supporting Information for

Electronic and Morphological Dual Modulation of Cobalt Carbonate Hydroxides by Mn Doping towards Highly Efficient and Stable Bifunctional Electrocatalysts for Overall Water Splitting

Tang Tang,[†,§,▽] Wen-Jie Jiang,[†,∥,▽] Shuai Niu,[†] Ning Liu,[‡,∥] Hao Luo,[†] Yu-Yun Chen,[†] Shi-Feng Jin,[‡,∥] Feng Gao,*[,§] Li-Jun Wan,[†,∥] Jin-Song Hu*[,†,∥]

[†]CAS Key Laboratory of Molecular Nanostructure and Nanotechnology, CAS Research/Education Center for Excellence in Molecular Sciences, Institute of Chemistry, Chinese Academy of Sciences, Beijing 100190, China

[§]Laboratory of Functionalized Molecular Solids, Ministry of Education, Anhui Key Laboratory of Chemo/Biosensing, Laboratory of Optical Probes and Bioelectrocatalysis, College of Chemistry and Materials Science, Anhui Normal University, Wuhu 241000, China

[‡]Research & Development Centre for Functional Crystals, Beijing National Laboratory for Condensed Matter Physics, Institute of Physics, Chinese Academy of Sciences, Beijing 100190, China

[∥]University of the Chinese Academy of Sciences, Beijing 100049, China

[▽]These authors contributed equally.

Corresponding Author

*fgao@mail.ahnu.edu.cn

*hujs@iccas.ac.cn

This file includes Figure S1-S22, and Table S1-S4.

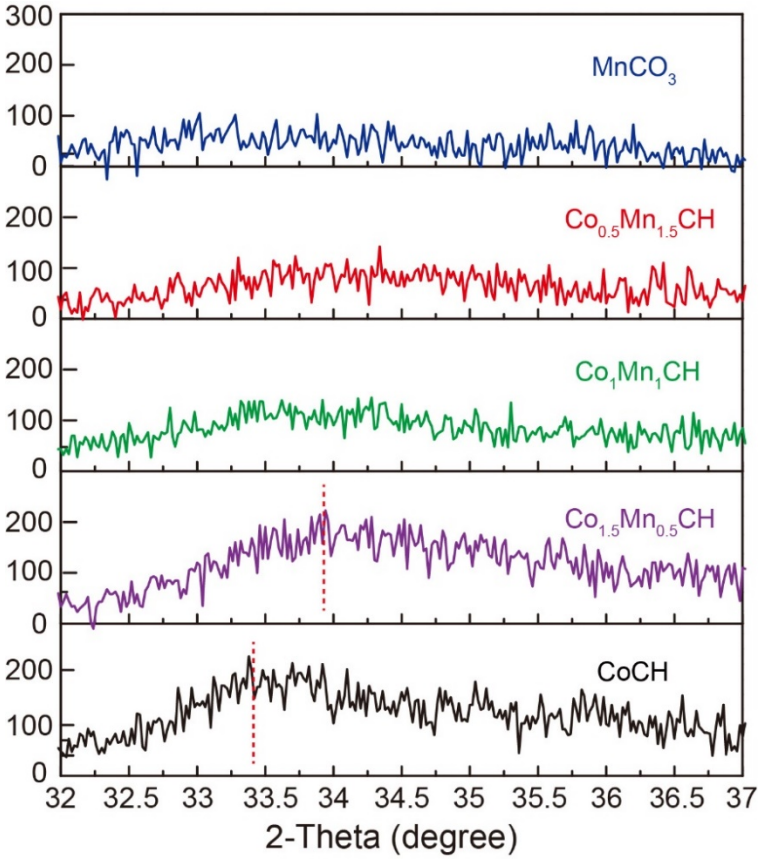

Figure S1. Enlarged XRD patterns of Co_xMn_yCH samples

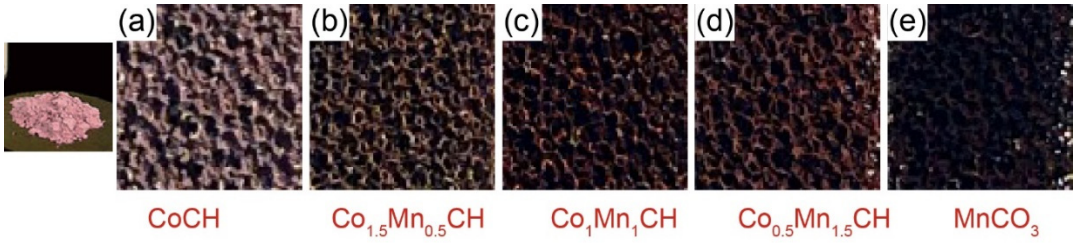

Figure S2. Photographs of (a) CoCH, (b) $Co_{1.5}Mn_{0.5}CH$, (c) Co_1Mn_1CH, (d) $Co_{0.5}Mn_{1.5}CH$, and (e) $MnCO_3$ on nickel foam. The picture on the left of (a) is cobalt carbonate hydroxide powder from network. The color of CoCH is similar to cobalt carbonate hydroxide powder, suggesting the formation of cobalt carbonate hydroxide. As the Mn feeding ratio increased, the pink color of the obtained products gradually faded away and became dark black for $MnCO_3$, agree with the color of manganese carbonate.

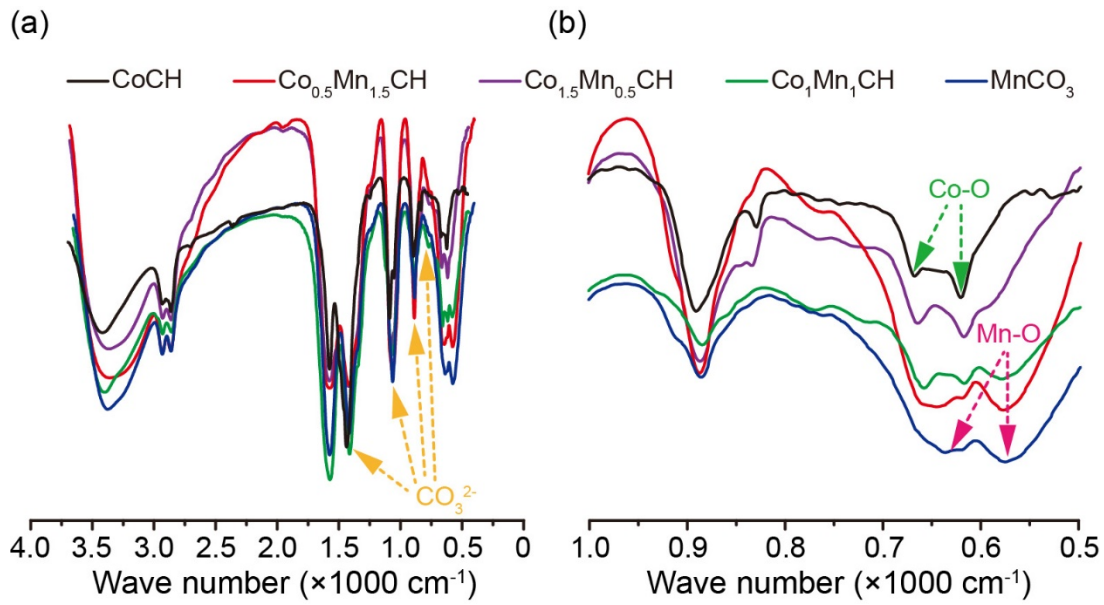

Figure S3. FTIR spectra of Co_xMn_yCH samples.

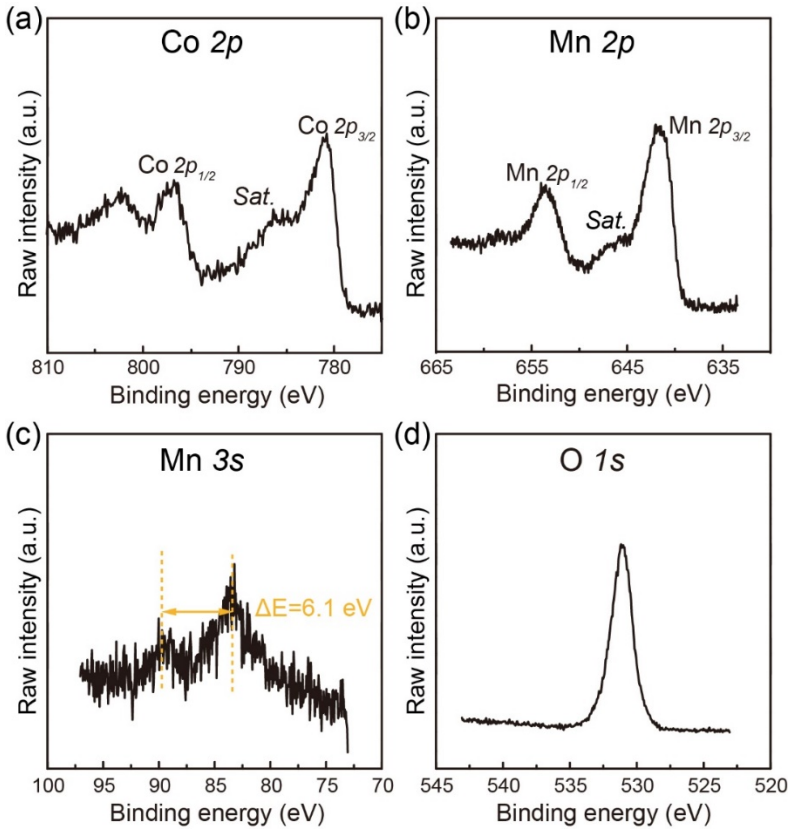

Figure S4. XPS spectra of (a) Co *2p*, (b) Mn *2p*, (c) Mn *3s*, and (d) O *1s* for Co_1Mn_1CH.

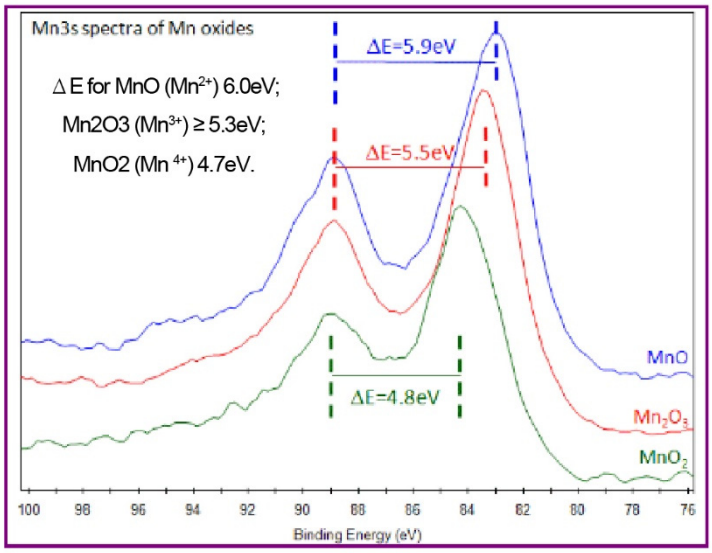

Figure S5. Standard Mn *3s* spectra for Mn in different chemical valences obtained from Avantage software as references.

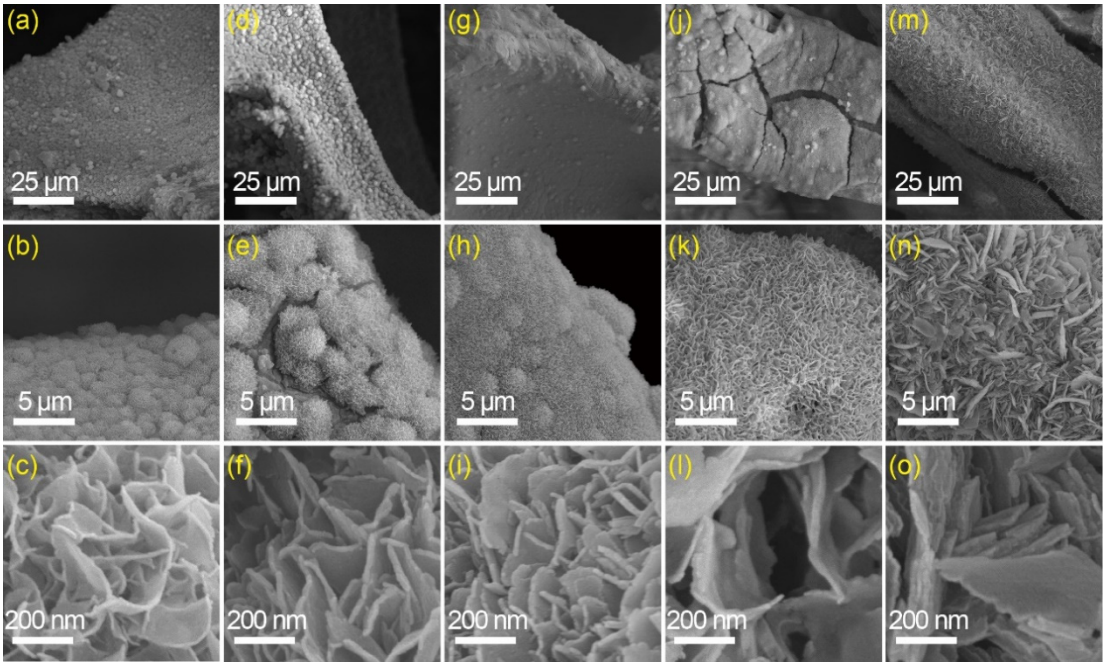

Figure S6. SEM images at various magnifications of (a-c) CoCH, (d-f) $Co_{1.5}Mn_{0.5}CH$, (g-i) Co_1Mn_1CH, (j-l) $Co_{0.5}Mn_{1.5}CH$, and (m-o) $MnCO_3$.

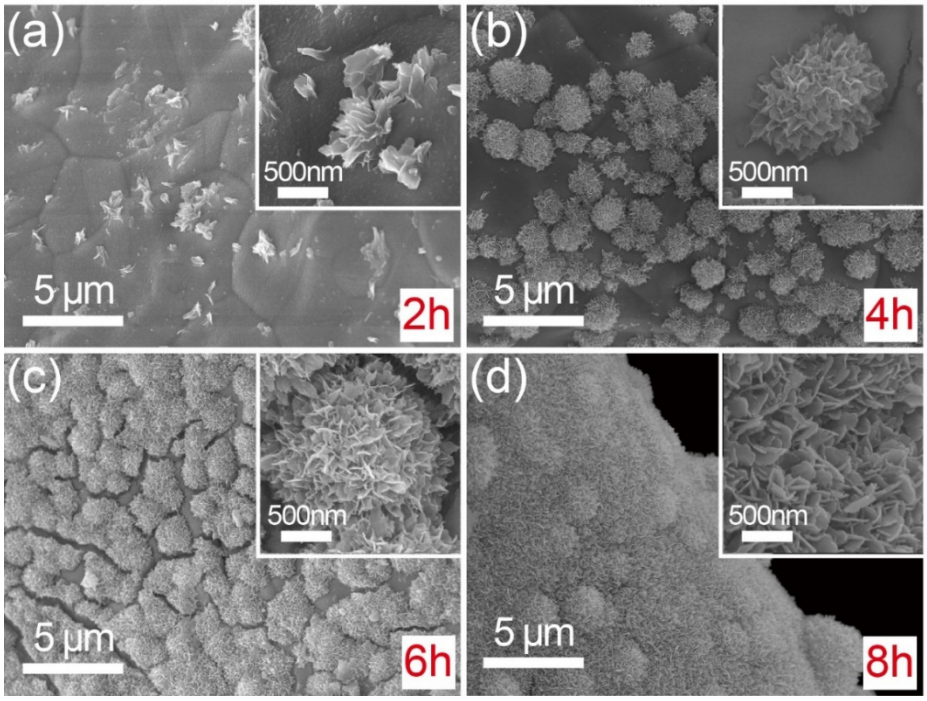

Figure S7. SEM images of Co_1Mn_1CH samples collected at the different reaction stages. All the insets are the corresponding SEM images at higher magnification.

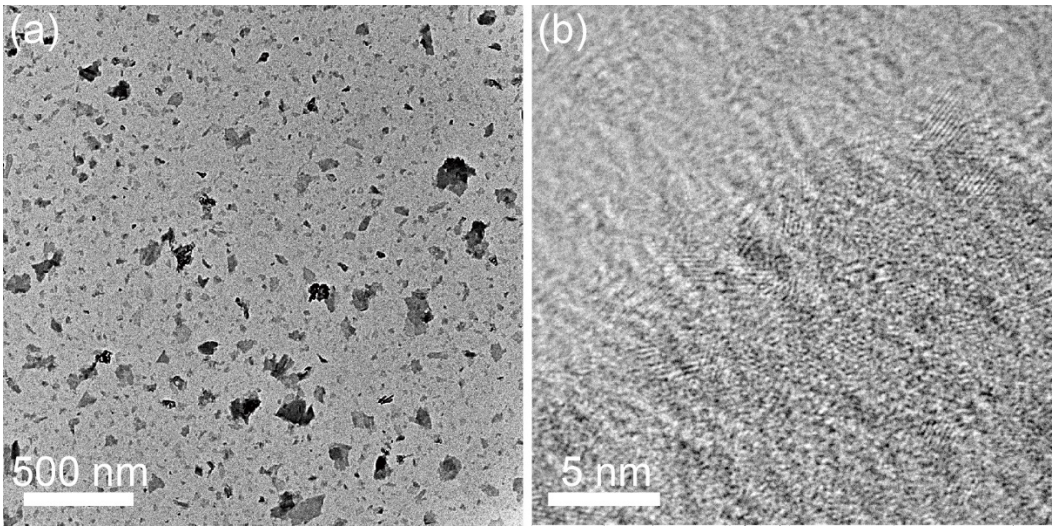

Figure S8. (a) TEM and (b) HRTEM images of Co_1Mn_1CH sample.

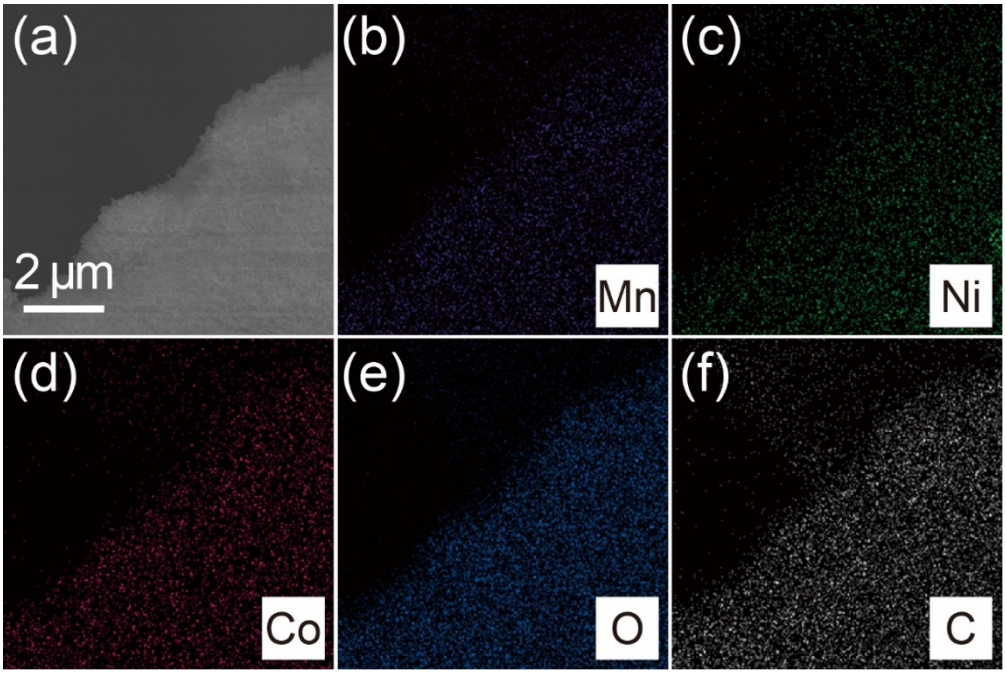

Figure S9. The morphology and the corresponding EDS mapping images of Co_1Mn_1CH collected on SEM.

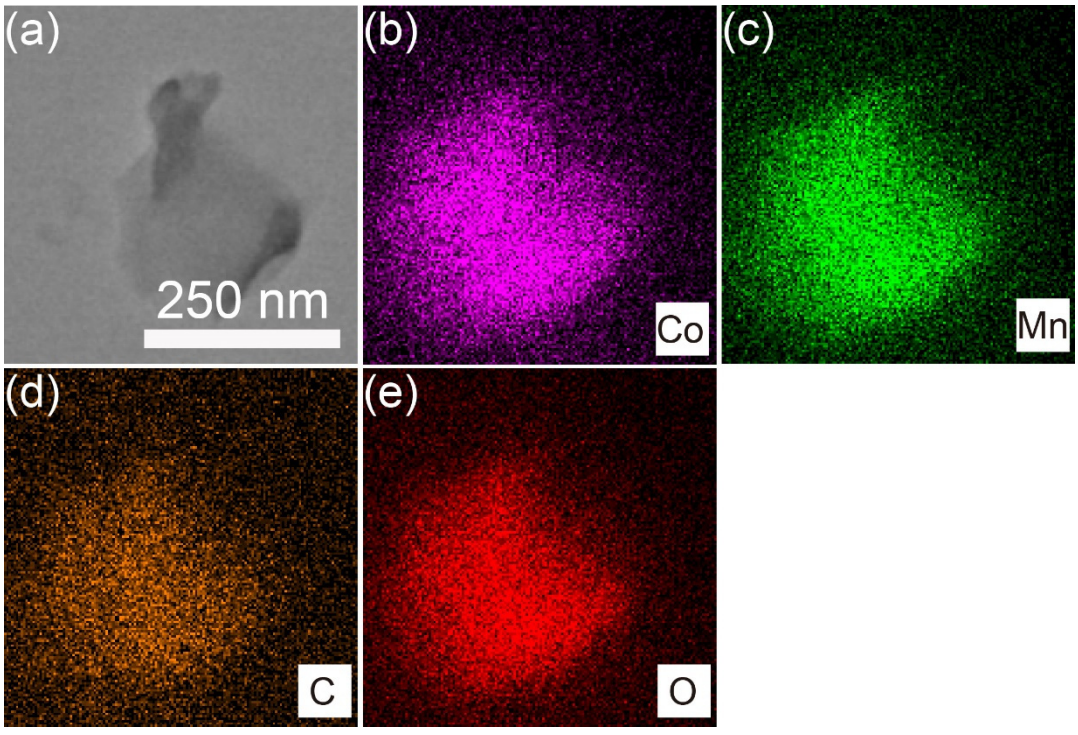

Figure S10. The morphology and the corresponding EDS mapping images of a single Co_1Mn_1CH nanosheet collected on TEM.

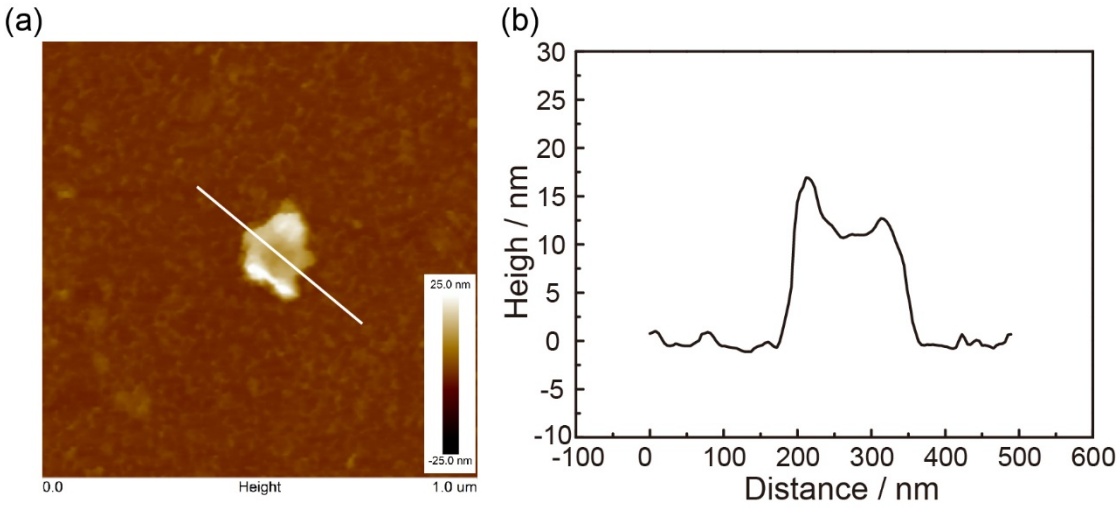

Figure S11. (a) Tapping mode AFM image of a single Co_1Mn_1CH nanosheet and (b) the corresponding height profile as marked by the line in (a).

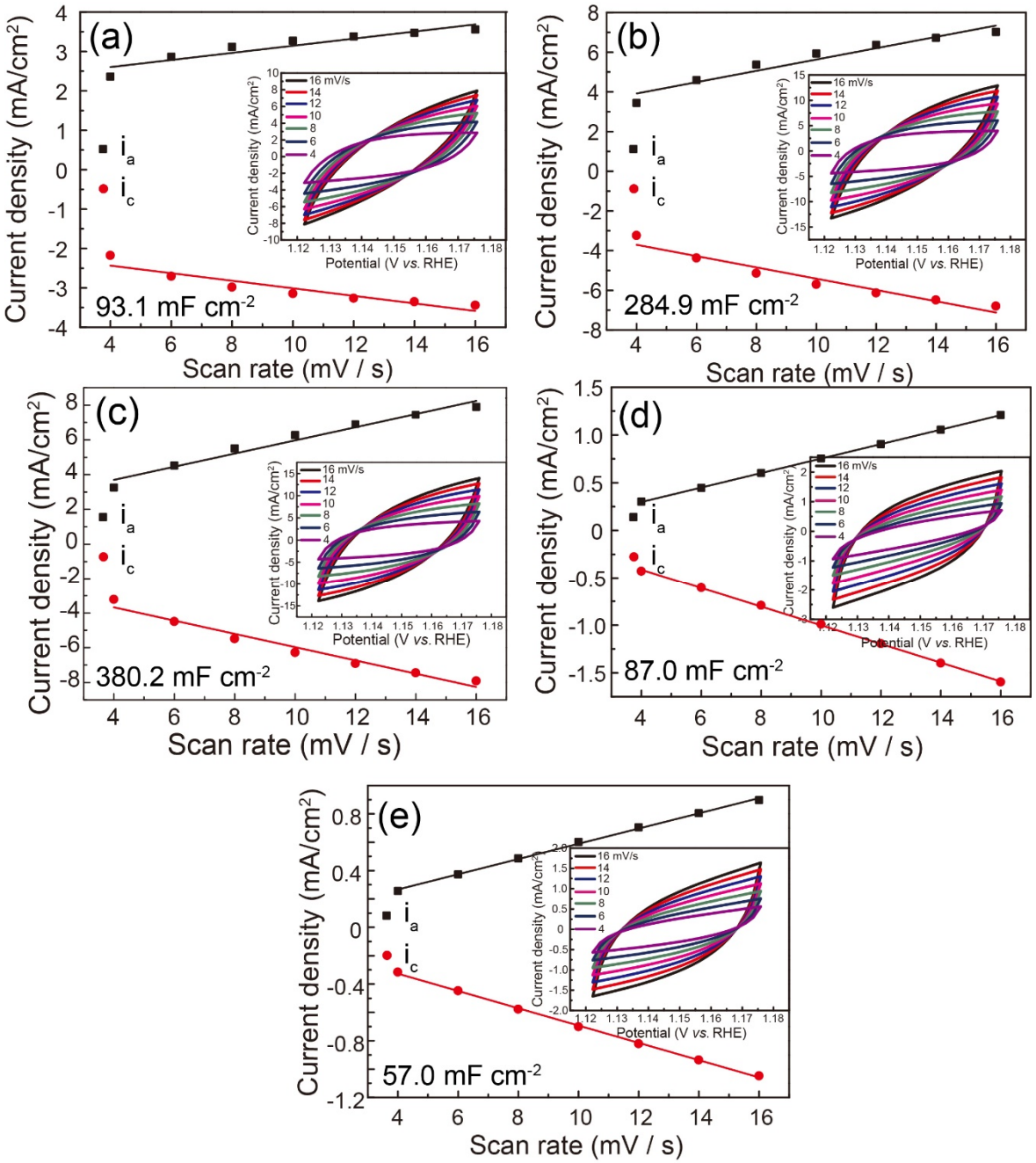

Figure S12. The plots of current density as a function of scan rates for **(**a) CoCH, (b) $Co_{1.5}Mn_{0.5}CH$, (c) Co_1Mn_1CH, (d) $Co_{0.5}Mn_{1.5}CH$, and (e) $MnCO_3$. The insets are the corresponding cyclic voltammograms at various scan rates of 4, 6, 8, 10, 12, 14, and 16 mV s^{-1}.

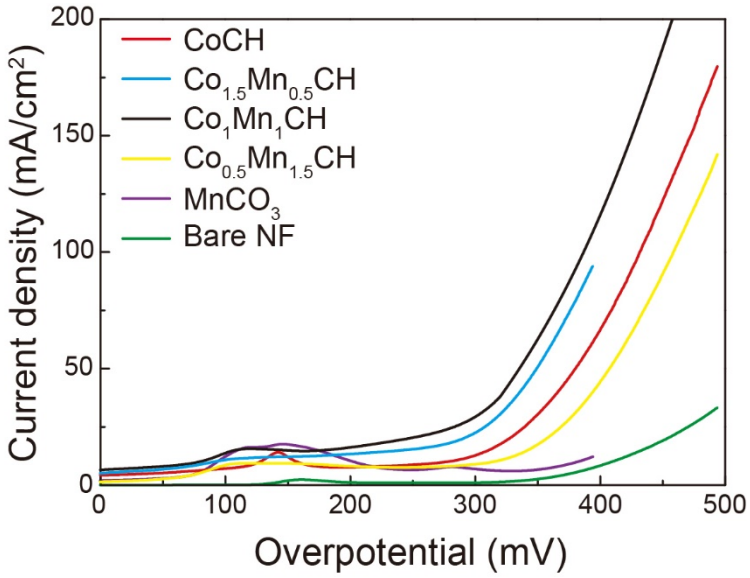

Figure S13. OER polarization curves without iR-compensation for Co_xMn_yCH samples at a scan rate of 5 mV s^{-1}.

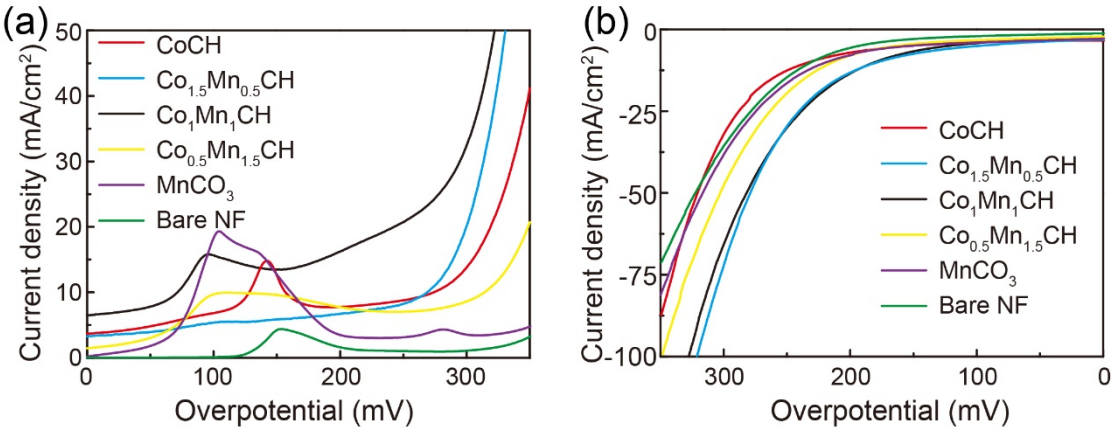

Figure S14. Enlarged (a) OER and (b) HER polarization curves of Co_xMn_yCH and bare NF in 1 M KOH at a scan rate of 5 mV s^{-1}.

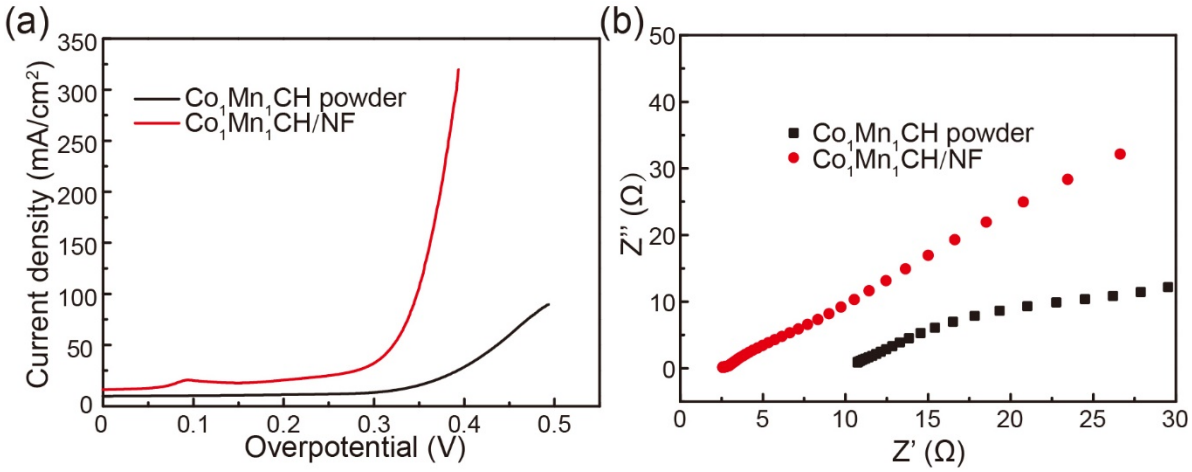

Figure S15. (a) OER polarization curves and (b) EIS Nyquist plots of Co_1Mn_1CH powder and Co_1Mn_1CH/NF at OCP condition.

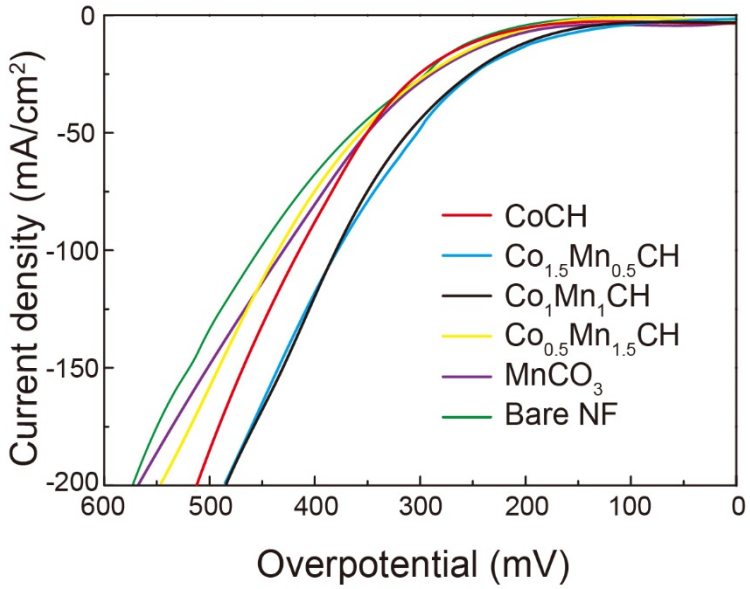

Figure S16. HER polarization curves without iR-compensation for Co_xMn_yCH samples at a scan rate of 5 mV s^{-1}.

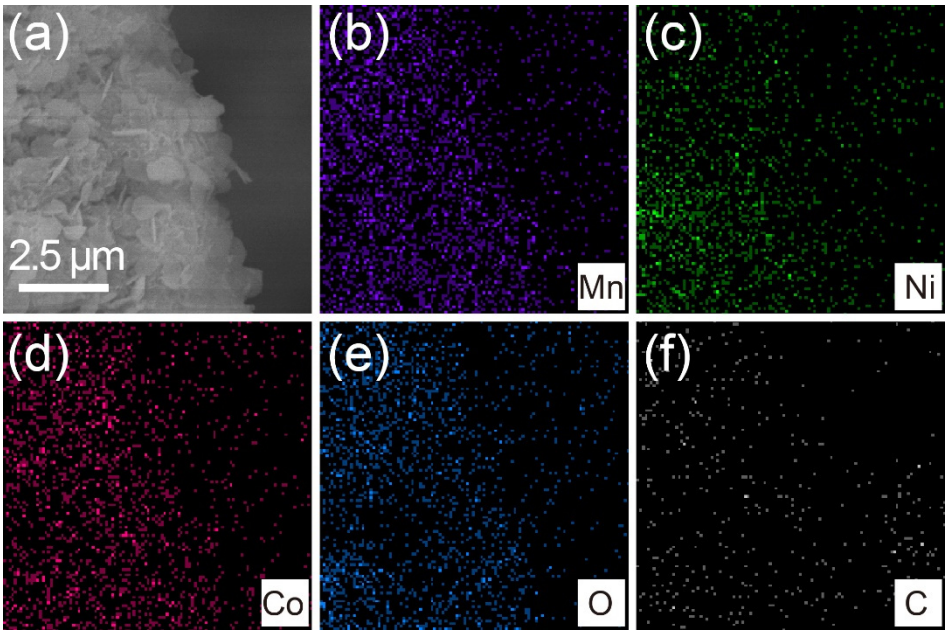

Figure S17. The morphology and the corresponding EDS mapping images of Co_1Mn_1CH after durability test.

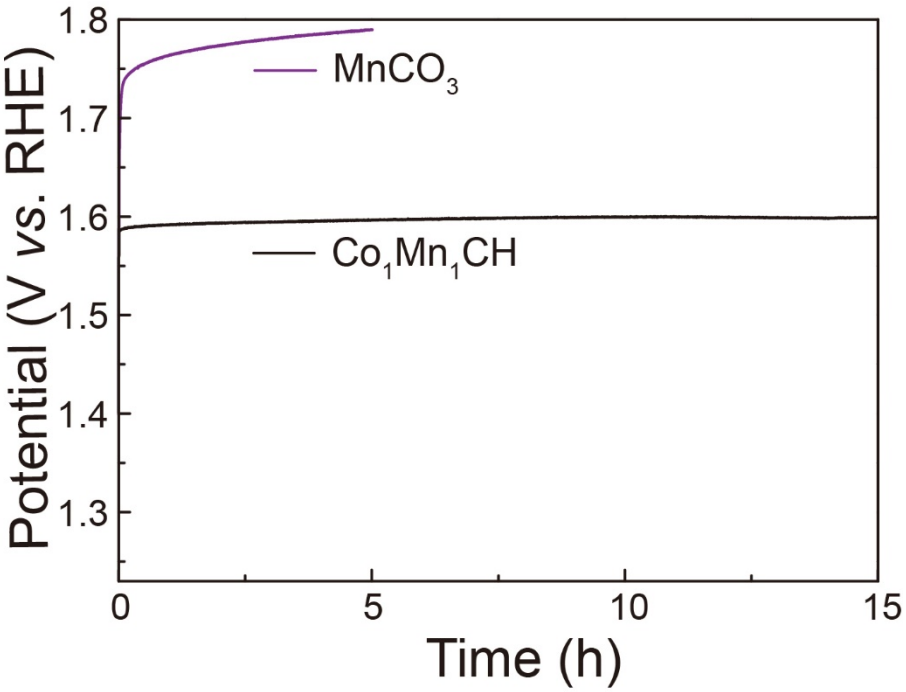

Figure S18. Chronopotentiometric curves of Co_1Mn_1CH and $MnCO_3$.

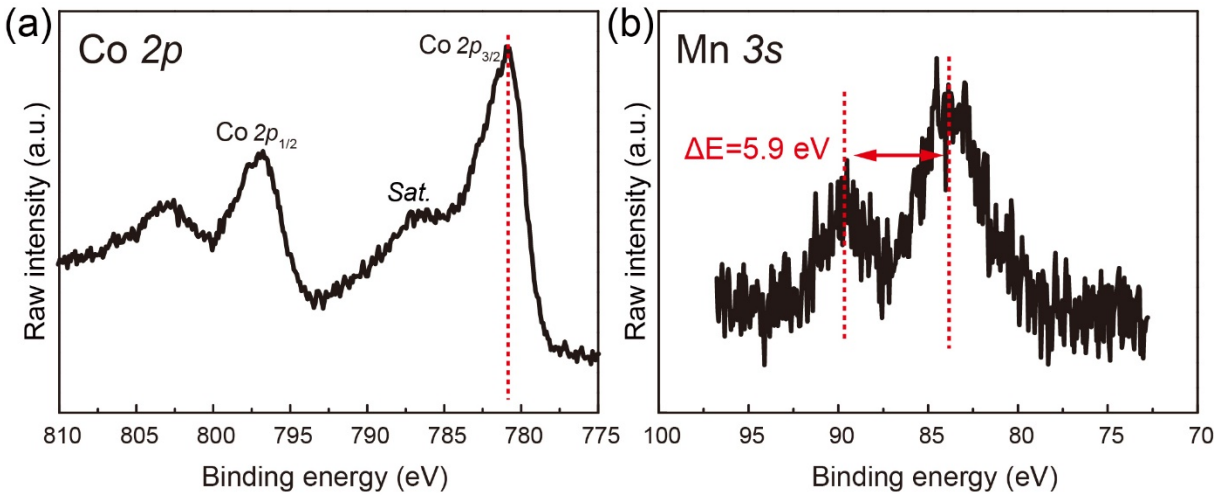

Figure S19. XPS spectra of (a) Co *2p* and (b) Mn *3s* for CoMnCH-ce.

Discussion on the chemical states of Co and Mn in CoMnCH-ce.

Both the peak of Co $2p_{3/2}$ at 780.9 eV and obvious shake-up peak at 785.0 eV are the same as those for Co_1Mn_1CH. As for the chemical state of Mn, ΔE of two Mn *3s* peaks is 5.9 eV, which is close to the value of 6.1 for Co_1Mn_1CH and suggesting bivalent Mn^{2+} in CoMnCH-ce, same as Co_1Mn_1CH. These results indicate that the similar electronic modulation on Co^{2+} was achieved by Mn doping via cation exchange versus the addition of Mn source during reaction.

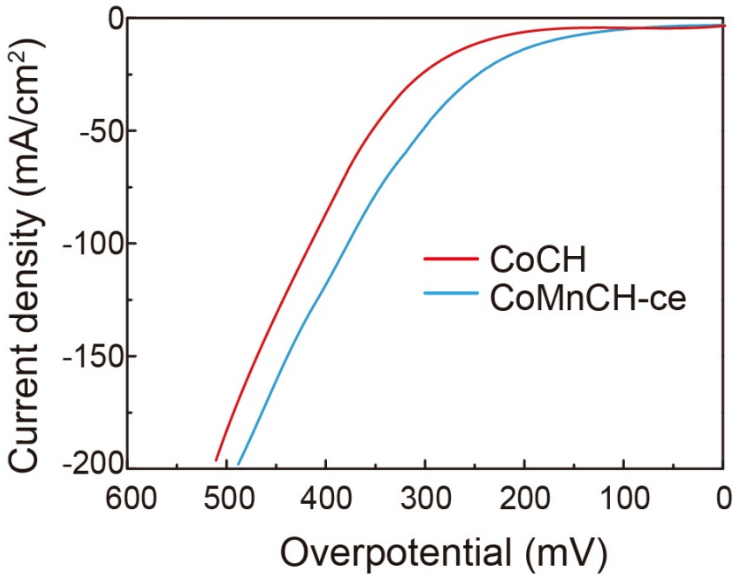

Figure S20. HER polarization curves without iR-compensation of CoCH and CoMnCH-ce.

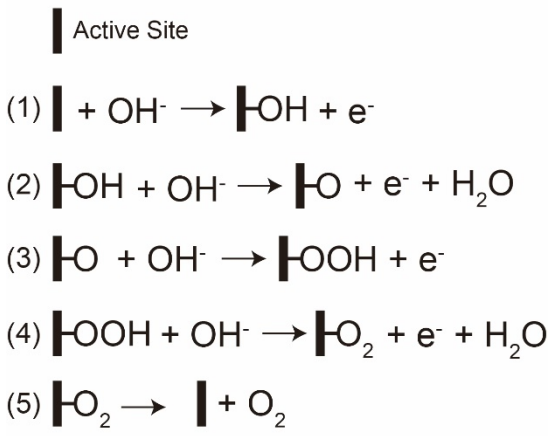

Figure S21. A schematic diagram depicting the general mechanism for electrochemical oxygen evolution reaction in basic solution.

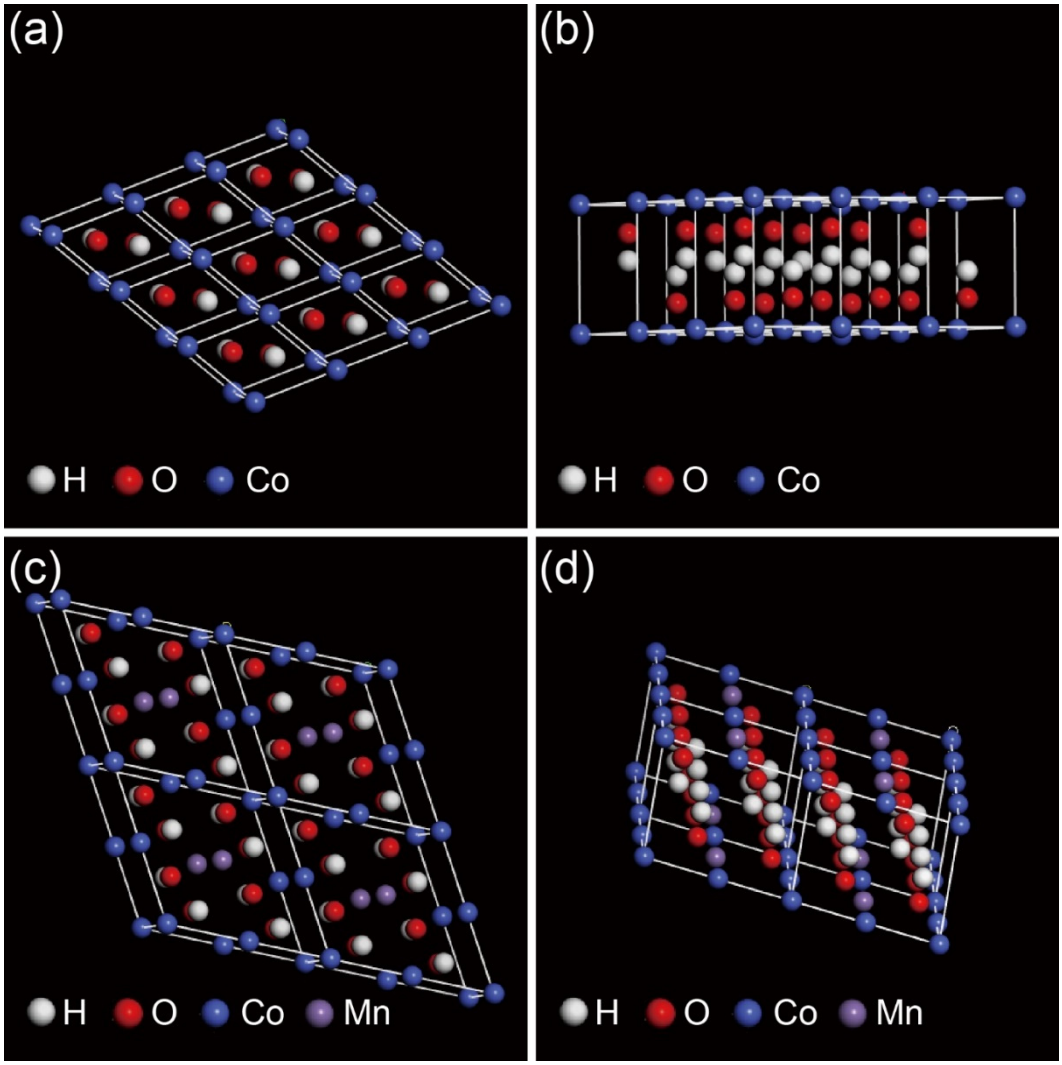

Figure S22. Crystal structure of (a-b) CoCH and (c-d) CoMnCH.

Table S1. The metal ratios of in Co_xMn_yCHs determined by EDS

Samples	**Elemental ratios / at.%**	
	Co	Mn
CoCH	100	-
$Co_{1.5}Mn_{0.5}CH$	72	28
Co_1Mn_1CH	51	49
$Co_{0.5}Mn_{1.5}CH$	29	71
$MnCO_3$	-	100

Table S2. Comparison of OER performance for the recently reported materials and ours.

Catalyst	Overpotential at current density of (mV)			Ref.
	10 mA cm^{-2}	50 mA cm^{-2}	100 mA cm^{-2}	
Co_1Mn_1CH*	-	322	349	**This work**
IrO_2	350	~ 400	~ 470	**Chem. Comm.** 2014, *50*, 13019
Co phosphide /phosphate	300	-	-	**Adv. Mater.** 2015, *27*, 3175.
NiFe LDH/NF	240	~ 350	~ 460	**Science** 2014, *345*, 1593.
Ni_5P_4*	~323	-	-	**Angew. Chem. Int. Ed.** 2015, *54*, 12361.
Co-CoO_x/CN*	260	~ 360	-	**J. Am. Chem. Soc.** 2015, *137*, 2688.
$NiCo_2O_4$*	290	~330	~360	**Angew. Chem. Int. Ed.** 2016, *55*, 6290.
$La_{0.3}(Ba_{0.5}Sr_{0.5})_{0.7}Co_{0.8}Fe_{0.2}O_{3-\delta}$*	~400 (0.1 M KOH)	-	-	**Angew. Chem. Int. Ed.** 2014, *53*, 4582
Co-P/NC*	319	-	-	**Chem. Mater.** 2015, *27*, 7636.
$NiCo_2O_4$/NF*	-	420	470	**Adv. Funct. Mater.** 2016, *26*, 4661.

* The overpotentials are given with iR-compensation.

Table S3. Comparison of HER performance for the recently reported materials and ours.

Catalyst	Overpotential at current density of (mV)			Ref.
	10 mA cm^{-2}	50 mA cm^{-2}	100 mA cm^{-2}	
Co_1Mn_1CH*	180	281	328	**This work**
$Pr_{0.5}(Ba_{0.5}Sr_{0.5})_{0.5}Co_{0.8}Fe_{0.2}O_{3-\delta}$*	237	~290	~310	**Adv. Funct. Mater.** 2016, *28*, 6442.
$NiCo_2O_4$/NF*	164	~250	~275	**Adv. Funct. Mater.** 2016, *26*, 3515.
Co phosphide /phosphate	380	-	-	**Adv. Mater.** 2015, *27*, 3175.
NiFe LDH/NF*	210	320	-	**Science** 2014, *345*, 1593.
Ni_5P_4*	150	-	-	**Angew. Chem. Int. Ed.** 2015, *54*, 12361.
Co-CoO_x/CN*	235	~350	-	**J. Am. Chem. Soc.** 2015, *137*, 2688
Co-P/NC	154	-	-	**Chem. Mater.** 2015, *27*, 7636.
$NiCo_2O_4$ NA/CC*	456	-	-	**Nanoscale** 2015, *7*, 15122.
$NiCo_2S_4$ NA/CC*	263	305	-	
$NiCo_2O_4$*	110	-	245	**Angew. Chem. Int. Ed.** 2016, *55*, 6290.
MoS_2/RGO*	~180	-	-	**J. Am. Chem. Soc.** 2011, *133*, 7296

* The overpotentials are given with iR-compensation.

Table S4. Comparison of overall water splitting performance for the recently reported materials and ours.

Catalyst	Potential at 10 mA cm^{-2} (V)	Ref.
Co_1Mn_1CH	1.68	**This Work**
NiFe LDH/NF	1.7	**Science** 2014, *345*, 1593.
Ni_5P_4	1.7	**Angew. Chem. Int. Ed.** 2015, *54*, 12361.
Co-CoO_x/CN	1.6	**J. Am. Chem. Soc.** 2015, *137*, 2688.
Co-P/NC	1.71	**Chem. Mater.** 2015, *27*, 7636.
$NiCo_2O_4$/NF	1.84	**Adv. Funct. Mater.** 2016, *26*, 4661.
$NiCo_2O_4$	1.65	**Angew. Chem. Int. Ed.** 2016, *55*, 6290.